

Efficient Land-cover Segmentation Using Meta Fusion

Hadi Mahdipour Hossein Abad*

Department of Marine Engineering, Khorramshahr University of Marine Science and Technology, Khorramshahr, Iran
mahdipour@kmsu.ac.ir

Morteza Khademi

Electrical Engineering Department, Ferdowsi University of Mashhad, Mashhad, Iran
khademi@um.ac.ir

Hadi Sadoghi Yazdi

Computer Engineering Department, Ferdowsi University of Mashhad, Mashhad, Iran
h-sadoghi@um.ac.ir

Received: 03/Mar/2015

Revised: 20/Jul/2016

Accepted: 25/Jul/2016

Abstract

Most popular fusion methods have their own limitations; e.g. OWA (order weighted averaging) has “linear model” and “summation of inputs proportions in fusion equal to 1” limitations. Considering all possible models for fusion, proposed fusion method involve input data confusion in fusion process to segmentation. Indeed, limitations in proposed method are determined adaptively for each input data, separately. On the other hand, land-cover segmentation using remotely sensed (RS) images is a challenging research subject; due to the fact that objects in unique land-cover often appear dissimilar in different RS images. In this paper multiple co-registered RS images are utilized to segment land-cover using FCM (fuzzy c-means). As an appropriate tool to model changes, fuzzy concept is utilized to fuse and integrate information of input images. By categorizing the ground points, it is shown in this paper for the first time, fuzzy numbers are need and more suitable than crisp ones to merge multi-images information and segmentation. Finally, FCM is applied on the fused image pixels (with fuzzy values) to obtain a single segmented image. Furthermore mathematical analysis and used proposed cost function, simulation results also show significant performance of the proposed method in terms of noise-free and fast segmentation.

Keywords: Fusion; Land-cover Segmentation; Multiple High-spatial Resolution Panchromatic Remotely Sensed (HR-PRS) Images; Fuzzy C-means (FCM).

1. Introduction

An important task in remote sensing (RS) applications is categorization of image pixels into homogeneous regions, whereas each of them corresponds to a particular land-cover type. This problem has often been modeled as **segmentation** problem and one of most utilized method to solve it, is clustering [1]. Nowadays land-cover segmentation using RS images, especially high-spatial resolution panchromatic remotely sensed (HR-PRS) ones (because of their high spatial resolution), becomes a challenging research task, due to this fact that objects in the unique scene (land-cover) often appear dissimilar in different RS images and sometimes incorrect (in someone) [2], though the land-cover has not changed. Generally obtained pixels values in RS images will be different with reality, which can be measurable by spectrometer in the ground field test, due to the following reasons:

- In the state of not being so obvious and where the (radiometric and geometric) preprocessing cannot model and remove sensor and atmosphere defects completely, the difference will be categorized as an un-sensible noise, caused by un-compensated sensor and atmosphere factors.
- On the other hand, if it happen the difference to be noticeable, as a matter of changes such as placing in

shadow or white cloudy dots, it is called unexpected noise.

On the other hand, by review the related papers to RS, it is observed there are two types of uncertainties in panchromatic images. The spatial uncertainty, as the famous one, imply to this fact that there is no an exact crisp separation between various land-covers types and the segments boundaries usually express softly continuous and using fuzzy sets [3-13]. The other uncertainty in RS images is the inherent one that imply to the inaccuracy and problems in sensing and digitizing the real phenomena [7]. There are two methods parametric and deterministic to model and analysis of inherent uncertainty. In the parametric one, the uncertainty is modeled using probability density function (pdf) [14-15]. Difficulty in allocating a pdf to a pixel and un-independence of neighborhood pixels are some problems of parametric method utilizing in RS applications [10,16,17]. In the deterministic method that is used in this paper, a symbolic interval number is used (instead of crisp one) to model the inherent uncertainty [18-20].

Utilization of **multiple RS images** to measure the ground physical and geometrical properties is a conventional way to overcome the uncertainty too [21-23]. Essentially, the concern of multi-images (multi-sensors) segmentation is minimizing the uncertainty. Furthermore,

* Corresponding Author

advantage of sharing various satellites data for using their capabilities simultaneously, encourages researchers to make use of multiple RS images. In this paper **HR-PRS images** are chosen to be utilized in land-cover segmentation because of their availability for us. Although by availability of other RS images (such as multi-spectral or even hyper ones), they can be used in the same procedure to land-cover segmentation too.

On the other hand, **Data fusion** is an effective way for optimum utilization of large volume data and combines different pieces of information into some new compatible information or more accurate data [24]. Application of data fusion methods varies a lot from military applications (such as target tracking and target recognition) to non-military ones (for example machine vision, robotics and medical). Data fusion tries to perform: 1) fusion of temporal information or 2) fusion of dissimilar information and or 3) fusion of similar information from different sources (or in fixed sensing object, fusion of information obtained by one unique sensor in various conditions and times) [24]. The first two categories are examined extensively in RS applications, named as multi-temporal [25] and conventional RS images fusion (producing high-resolution multispectral images from a high-resolution panchromatic image and a low-resolution multispectral image) [3] respectively. Despite that, there have not been many works for the third category, which is the category of proposed method in this paper. **RS images fusion** can be performed at three different processing levels, according to the stage at which the fusion takes place: pixel level, feature level, and decision level [25,26]. The fusion-based multi-images segmentation methods usually perform the fusion in pixel or decision level. In the pixel level fusion-based multi-images segmentation methods that is used in this paper, by create a new fused image from input images, it is tried to improve the segmentation accuracy [25].

Since the purpose of this paper is noise-free and correct segmentation, the multi-image segmentation using fusion method (in the pixel level) is concern of this paper. Although there are many new researches in the land-cover segmentation using a single RS image (for example see [27,28]), but no new method in multi-images segmentation has been clarified. Inspecting **multi-images segmentation**, two groups of researchers published some papers [21-23,29-33]. The first group (Lee et.al. [21-23]) integrated the data from individual sensors into a set of multidimensional data to segmentation using hierarchical clustering. Against, Pieczynski et al (the second group) [29-33] used hidden Markov model (HMM) to land-cover segmentation using multi RS images.

Generally the conventional fusion methods (for example let HMM, Kalman filter, order weighted averaging (OWA) or etc.), where they are used for multi-images segmentation, let a specific proportion for each input image in the fusion process (or in the final fused image), for all pixels. While this proportion must be certificated for each pixel separately based on this fact that ambiguity in the available values of the pixel is high

or low. Indeed since fuzzy concept can model existent inherent diversity and ambiguity in the available values for each land-cover point as well, the proposed method in this paper fuses the input images in one fuzzy image (an image that its pixels have fuzzy numbers instead of crisp ones). Finally the fuzzy c-means (FCM), as a commonly clustering method and a method with fuzzy output to model the spatial uncertainty, is applied on the fuzzy fused image pixels to obtain a single segmented image for each land-cover. The mathematical analysis show better performance of the proposed method in compare to the classical methods and conventional fusion methods. This is performed using a new proposed cost function. Simulation results confirm the efficiency of the proposed method in noise-free and fast segmentation aspects.

The **remainder of this paper** is organized as follows. The motivation of this paper, as a preface to understand the necessity of using non-crisp (fuzzy) numbers in land-cover segmentation using HR-PRS images is obtained in section 2. Section 3 introduces some preliminaries including the FCM clustering algorithm where it is applied on crisp and non-crisp numbers. Section 4 presents the proposed method to land-cover segmentation using multiple co-registered panchromatic images. Furthermore some analyses and comparisons are obtained in section 4 too. Simulation results are obtained in Section 5. Finally this paper is concluded in Section 6.

2. Motivation

In this section, as a preface to understand the necessity of using non-crisp (fuzzy) numbers in land-cover segmentation using RS images, land-cover points are categorized according to available multi RS images from that land-cover (for the first time). For simplicity this work is performed for images (HR-PRS ones) and based on spectral feature in this paper; however it can be performed for other signals (except image) and based on other (non-spectral) image features similarly.

Let the actual value of under-studying land-cover points (n points) in the studied feature (gray-scale level) be denoted by $\tilde{X} = \{\tilde{x}_1, \dots, \tilde{x}_k, \dots, \tilde{x}_n\}$, which can be achieved using spectrometer in ground field test. Considering unavailability of these values (because of unperforming ground field experiments) and the range of numbers which can be specified to each segment of land-cover (for example let a river as a segment that its pixels values vary with depth of water, water impurity, kind of river bottom and etc.), an interval is considered for the actual value of each pixel ($\tilde{x}_k \in [\tilde{x}_k^{\min}, \tilde{x}_k^{\max}]$, $k = 1, \dots, n$).

Letting L available (co-registered) HR-PRS images ($X^{(l)} = \{x_1^{(l)}, \dots, x_k^{(l)}, \dots, x_n^{(l)}\}$, $l = 1, \dots, L$), It is observed that, nevertheless the covered land-cover by all L images and even the used sensor for imaging may be same, but most corresponding pixels in L images have different values. This phenomenon can be seen easily in the first scene images and Figure 1 that are obtained using IRS-P5

satellite. Comparing values of first scene images, pixel by pixel, it can be observed that only 0.84% of pixels have same values in both images, for 62.54% of pixels, image A and for the remainder (36.61%), image B has more values (e.g. under shadow region of image A, mentioned by circle). Therefore, the minimum and maximum of observed values sets can be defined as follows:

$$X^{\min} = \{x_1^{\min}, \dots, x_n^{\min}\} \text{ where } x_k^{\min} = \min\{x_k^{(1)}, \dots, x_k^{(L)}\} \text{ for } k = 1, \dots, n \quad (1)$$

$$X^{\max} = \{x_1^{\max}, \dots, x_n^{\max}\} \text{ where } x_k^{\max} = \max\{x_k^{(1)}, \dots, x_k^{(L)}\} \text{ for } k = 1, \dots, n \quad (2)$$

According to above notes and also considering the variation of $x_k^{(l)}$ and \check{x}_k ($x_k^{(l)} \in [x_k^{\min}, x_k^{\max}]$ and $\check{x}_k \in [\check{x}_k^{\min}, \check{x}_k^{\max}]$) each point of land-cover will belong to one of two following categories based on the relation between actual values range ($[\check{x}_k^{\min}, \check{x}_k^{\max}]$) and range of obtained values by L images ($[x_k^{\min}, x_k^{\max}]$).

- First category land-cover points are not influenced by unwanted and unexpected happenings (such as placing under white cloudy dot or in the shadow region) in the input images. Since the (radiometric and geometric) preprocessing cannot model and remove sensor and atmosphere defects completely, this category is affected only by un-modeled (or more precisely, weak modeled) causes of sensor and atmosphere, named as un-sensible noise in this paper. The considered model for atmosphere, compose of various probability distributions (for example see [34]), is an acceptable reason for this fact that atmosphere defect cannot be removed from RS images completely. Therefore the relations between variation ranges of $x_k^{(l)}$ and \check{x}_k for each point of this category will be one of nine states Figure 2-A. For this group of pixels, the actual value \check{x}_k ($\check{x}_k \in [\check{x}_k^{\min}, \check{x}_k^{\max}]$) is shown by bilateral black vector in Figure 2-A) is influenced by un-sensible noise. So the variation range of obtained values by input

images ($x_k^{(l)} \in [x_k^{\min}, x_k^{\max}]$) is shown by one sided blue vector in Figure 2-A) will be small and in the order of \check{x}_k variation range.

- Second group points are affected by un-wanted (un-expected) noise (e.g. placing in shadow or white cloudy dots) in addition un-sensible one, at least in one input image. This group of pixels is supposed to be affected by un-sensible noise as the simplest state (top-left state of Figure 2-A). Major reason of this assumption is more role of un-expected noise comparing the un-sensible one in the values of these pixels. The relation between the variations ranges of $x_k^{(l)}$ and \check{x}_k in this pixels categorization will be accessible through one of following three states, Figure 2-B:D.

According to the mentioned notes, a segmentation methodology must be selected that obtain noise-free labels (segments) for all land-cover points using multi-images, of which the pixels would have each states of Figure 2-A:D.

In the other view, according to relations (1) and (2), an n-dimensional hyper-cube can be defined as the input space in segmentation of land-cover using multi-images. The range of each dimension (for example the dimension k-th) is from x_k^{\min} to x_k^{\max} . For $n = 2$ this input space is illustrated in Figure 2-E.

According to above explanations (performed categorization) it can be concluded that it is very probable (except in $\check{x}_k \notin [x_k^{\min}, x_k^{\max}]$ cases) to present the actual values of land-cover points ($\check{X} = \{\check{x}_1, \dots, \check{x}_k, \dots, \check{x}_n\}$) by a point in this hyper-cube (inside it or on its boundary). This point which can be named as the **optimum point in the input space (OPIS)** is unknown when only RS images are used to segment and any ground truth data is not available. Obviously, applying the clustering method (e.g. FCM) on the OPIS, the optimum response (optimum centers and membership values and finally optimum segmented image) can be reached.

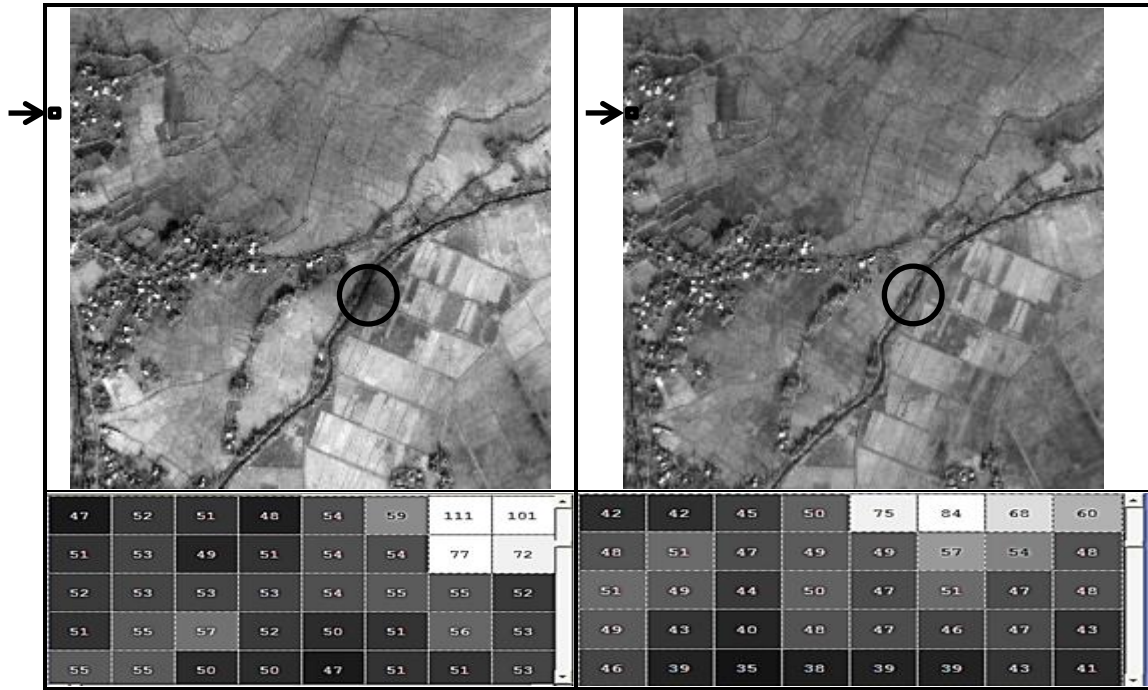


Fig. 1. The first land-cover images (left: A and right: B) and corresponding values of mentioned regions by \rightarrow .

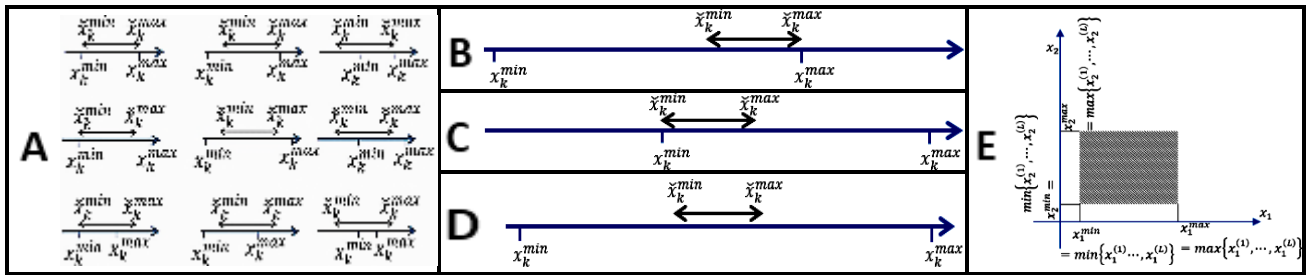


Fig. 2. The corresponding figures of land-cover points categorizing; the variation ranges of actual pixel number ($\tilde{x}_k \in [\tilde{x}_k^{\min}, \tilde{x}_k^{\max}]$ is shown by bilateral vector) and the obtained values by L input images for k-th pixel ($x_k^{(l)} \in [x_k^{\min}, x_k^{\max}]$ is shown by one sided vector), where in A it is influenced only by un-sensible noise in all L input images; in B it only is placed in shadow at least in one input image, in C it only is placed under white cloudy dot at least in one input image, in D it is placed in shadow and white cloudy dot at least in two separate input images; E. The input space of multi-images segmentation (hyper-cube for $n = 2$)

3. Preliminaries

In this section, as the proposed method is based on the conventional FCM, a description of FCM will be given concerning the special manner in which it is applied on crisp numbers. Then symbolic interval numbers as the simplest fuzzy numbers type along with the FCM applying on them, are explained.

3.1 FCM Algorithm and Crisp Numbers

The fuzzy c-means (FCM) algorithm, the best-known clustering algorithm, has been used in a wide range of engineering and scientific disciplines such as medicine imaging, bioinformatics, pattern recognition, and data mining [35,36]. FCM clustering method assigns fuzzy memberships to each input member. This method is fuzzy equivalence of the nearest center “hard” clustering method. The aim of FCM algorithm is minimizing the

following objective function ($J(U,V)$) with respect to fuzzy memberships $U = [u_{i,k}]_{c \times n}$ and cluster centers $V = \{v_1, \dots, v_i, \dots, v_c\}$,

$$J(U, V) = \sum_{i=1}^c \sum_{k=1}^n u_{i,k}^\theta d^2(x_k, v_i) \quad (3)$$

$$d^2(x_k, v_i) = (x_k - v_i)^T (x_k - v_i) = \|x_k - v_i\|^2 \quad (4)$$

Where n is the number of input numbers, c is the number of clusters, $X = \{x_1, \dots, x_k, \dots, x_n\}$ is the set of input numbers which is a finite set of p -dimensional vectors on the real numbers ($x_k = [x_{k,1}, \dots, x_{k,p}]^T \in \mathbb{R}^p$ for $k = 1, \dots, n$) and $\theta > 1$ is the fuzziness index. The matrix $U = [u_{i,k}]_{c \times n}$ is called the fuzzy membership degree with following constraint:

$$\begin{cases} u_{i,k} \in [0,1], \text{ for } i = 1, \dots, c \text{ and } k = 1, \dots, n \\ \sum_{i=1}^c u_{i,k} = 1, \quad k = 1, \dots, n \end{cases} \quad (5)$$

Where $u_{i,k}$ is the membership grade of k -th input number to i -th cluster. $V = \{v_1, \dots, v_i, \dots, v_c\}$ is the cluster prototypes (centers) set, $v_i = [v_{i,1}, \dots, v_{i,p}]^T \in \mathbb{R}^p$ for $i = 1, \dots, c$ is the center of i -th cluster and $d^2(x_k, v_i)$ denotes the Euclidean distance of x_k and v_i in p -dimensions space.

Creating Lagrange function $L(U, V, \lambda)$ and using Lagrange multipliers $\lambda_k, k = 1, \dots, n$, the objective function $J(U, V)$ can be minimized subject to constraints (5) to conclude updating relations as follows:

$$L(U, V, \lambda) = \sum_{i=1}^c \sum_{k=1}^n u_{i,k}^\theta d^2(x_k, v_i) - \sum_{k=1}^n \lambda_k \left(\sum_{i=1}^c u_{i,k} - 1 \right) \quad (6)$$

$$\partial L(U, V, \lambda) / \partial u_{i,k} = 0 \Rightarrow \dots \Rightarrow u_{i,k} = \left(\sum_{r=1}^c \frac{d^2(x_k, v_r)}{d^2(x_k, v_i)} \right)^{\frac{1}{\theta-1}} \quad (7)$$

$$\partial L(U, V, \lambda) / \partial v_i = 0 \Rightarrow \dots \Rightarrow v_i = \frac{\sum_{k=1}^n u_{i,k}^\theta x_k}{\sum_{k=1}^n u_{i,k}^\theta} \quad (8)$$

where $d^2(x_k, v_i) = (x_k - v_i)^T (x_k - v_i)$ is the euclidean distance of x_k and v_i and $i = 1, \dots, c$ and $k = 1, \dots, n$.

3.2 FCM Algorithm and Non-Crisp Numbers

Since for all studied scenes (land-covers) in this paper only two HR-PRS images are available and symbolic interval numbers are the best fuzzy (non-crisp) numbers to represent two available values of a fact (in this paper, each land-cover point), in this sub-section the symbolic interval numbers as the simplest non-crisp (fuzzy) numbers are introduced and discussed. A non-crisp number \tilde{x} will be supposed as a symbolic interval number (SIN) if its membership function be expressed as follows [37]:

$$\mu_{\tilde{x}}(x) = \begin{cases} 1 & , \alpha_{\tilde{x}} \leq x \leq \beta_{\tilde{x}} \\ 0 & , \text{Otherwise} \end{cases} \quad (9)$$

A SIN \tilde{x} can be denoted with its start point ($\alpha_{\tilde{x}}$) and its end point ($\beta_{\tilde{x}}$) as $\tilde{x} = (\alpha_{\tilde{x}}, \beta_{\tilde{x}})_{\text{SIN}}$.

Suppose two symbolic interval numbers \tilde{x}_k and \tilde{v}_i in p dimensions space, $\tilde{x}_k = \{\tilde{x}_{k,1}, \tilde{x}_{k,2}, \dots, \tilde{x}_{k,p}\}$, $\tilde{x}_{k,j} = (\alpha_{\tilde{x}_{k,j}}, \beta_{\tilde{x}_{k,j}})_{\text{SIN}}$ and $\tilde{v}_i = \{\tilde{v}_{i,1}, \tilde{v}_{i,2}, \dots, \tilde{v}_{i,p}\}$, $\tilde{v}_{i,j} = (\alpha_{\tilde{v}_{i,j}}, \beta_{\tilde{v}_{i,j}})_{\text{SIN}}$ for $j = 1, 2, \dots, p$. The used metric (dissimilarity or distance) for SINs in [37], as the simplest metric in the symbolic interval numbers case which is used in this paper, is as follows:

$$d^2(\tilde{x}_k, \tilde{v}_i) = \sum_{j=1}^p \left(\left(\alpha_{\tilde{x}_{k,j}} - \alpha_{\tilde{v}_{i,j}} \right)^2 + \left(\beta_{\tilde{x}_{k,j}} - \beta_{\tilde{v}_{i,j}} \right)^2 \right) \quad (10)$$

Based on above metric, the FCM can be applied on SINs as follows [37]:

$$\begin{aligned} & \underset{\tilde{V}, U}{\operatorname{argmin}} \quad \{J(\tilde{V}, U) = \sum_{i=1}^c \sum_{k=1}^n u_{i,k}^\theta d^2(\tilde{x}_k, \tilde{v}_i)\} \Rightarrow \dots \Rightarrow \\ & \text{subject to: } \sum_{i=1}^c u_{i,k} = 1 \quad , \quad \text{for } k = 1, \dots, n \\ & \left\{ \begin{aligned} u_{i,k} &= \left(\sum_{j=1}^c \frac{d^2(\tilde{x}_k, \tilde{v}_j)}{d^2(\tilde{x}_k, \tilde{v}_i)} \right)^{\frac{1}{\theta-1}} \\ \alpha_{\tilde{v}_{i,j}} &= \frac{\sum_{k=1}^n u_{i,k}^\theta \alpha_{\tilde{x}_{k,j}}}{\sum_{k=1}^n u_{i,k}^\theta} \\ \beta_{\tilde{v}_{i,j}} &= \frac{\sum_{k=1}^n u_{i,k}^\theta \beta_{\tilde{x}_{k,j}}}{\sum_{k=1}^n u_{i,k}^\theta} \end{aligned} \right. \quad (11) \end{aligned}$$

Having fulfilled the preliminaries, the proposed method will be presented in the next section.

4. Proposed Method

This section of paper proposes a land-cover segmentation algorithm using available multi HR-PRS images from the land-cover and compares it analytically with other methods in the following sub-sections.

4.1 Descriptions

The structure of the proposed method, containing 5 blocks, is as Figure 3 which will be explained consequently block by block.

HR-PRS input images: As mentioned, L HR-PRS images with same spatial-resolution are considered as input images. These images, registered together and denoted by $X^{(l)} = \{x_1^{(l)}, \dots, x_n^{(l)}\}, l = 1, \dots, L$ belong to same unchanged scene.

Pixels fuzzifying: As mentioned in introduction, the nature of proposed method and the considered problem in this paper differs with normal concept of RS images fusion [3]. But in the other view, the proposed method can be considered as a method to fuse multi HR-PRS images and applying the segmentation process on the fused image. On the other hand, fuzzy concept, in comparison with crisp one and in the way it was described, can represent land-cover points completely when multi images are available. Therefore the proposed method considers a fuzzy (non-crisp) number value for each fused image pixel. This fuzzy number is obtained using L available values for each land-cover point. The fuzzy number can be a symbolic interval type fuzzy one in the simplest state. LR-Type, Gaussian (normal), triangular, trapezoidal and etc. are other types of fuzzy numbers that can be used. Since, in this paper only two images are available for each land-cover ($L = 2$), based on two available values for each land-cover point, the small one is considered as x_k^{\min} and the other one as x_k^{\max} . Finally, each pixel in the fused image is demonstrated by $\tilde{x}_k = \tilde{x}_{k,\text{SIN}} = (\alpha_{\tilde{x}_k}, \beta_{\tilde{x}_k})_{\text{SIN}} = (x_k^{\min}, x_k^{\max})_{\text{SIN}}$, indeed, $\alpha_{\tilde{x}_k} = x_k^{\min}$ and $\beta_{\tilde{x}_k} = x_k^{\max}$.

FCM and Determine optimum clusters number:

let's suppose that we want to cluster the land-cover (fused image) to c ($c \geq 2$) clusters. The proposed method applies FCM on the fused image, just one time and according to the mentioned procedure in section (3.2), to obtain a single segmented image for each land-cover. As far as a mathematical based fusion concerns, the proposed method can be presented as follows:

$$\begin{aligned} \tilde{x}_k &= \text{Fusion}(x_k^{(1)}, \dots, x_k^{(l)}, \dots, x_k^{(L)}) \Rightarrow \\ \underset{\tilde{V}, U}{\text{argmin}} \quad & \{J(\tilde{V}, U) = \sum_{i=1}^c \sum_{k=1}^n u_{i,k}^\theta d^2(\tilde{x}_k, \tilde{v}_i)\} \\ \text{subject to: } & \sum_{i=1}^c u_{i,k} = 1, \text{ for } k = 1, \dots, n \end{aligned} \quad (12)$$

Where, the notation $\tilde{}$ is used to represent fuzzy (in this section, symbolic interval) numbers, n is the number of per input image pixels (or under-studying land-cover points), c is the number of clusters, $\tilde{V} = \{\tilde{v}_1, \dots, \tilde{v}_c\}$ and \tilde{v}_i is the center of i -th cluster, $d(\cdot)$ represents the distance of two SINs according to (10), $\theta > 1$ is the fuzziness index and the matrix $U = [u_{i,k}]_{c \times n}$ is called the fuzzy membership degree.

It must be mentioned, one of problems in image segmentation is obtaining optimum number of segments for each input land-cover [38]. In the clustering based segmentation methods, this is equivalent to optimum clusters number determination process (named OCNDP in this paper) for the fused image usually performed by optimizing a cluster validity index where varies with the number of clusters [39]. This paper uses Xie-Beni (XB) cluster validity index [40] for finding the optimum number of clusters. The XB index is defined as a function of total variation ratio to clusters' centers minimum separation as follows:

$$XB(c) = J / \left(\min_{i \neq j} \{d^2(v_i, v_j)\} \right) \quad (13)$$

Where, J is the minimized objective function by clustering algorithm, and v_i and v_j are two separate clusters centers.

Since the centers in the proposed method are non-crisp, v_i and v_j are replaced by \tilde{v}_i and \tilde{v}_j respectively in equation (13) and $d^2(\tilde{v}_i, \tilde{v}_j)$ is obtained using equation (10). Therefore, the optimum number of clusters \hat{c} can be achieved for each land-cover using the following equation:

$$\hat{c} = \underset{c}{\text{argmin}} XB(c) \quad (14)$$

As a result, outcomes of FCM applied on the fused image (where the number of clusters is \hat{c}) are considered to be the output of this block and consequently, input for the next block (Defuzzification).

Defuzzification: Having clustered fused image (to \hat{c} clusters), to assign the pixels to correspondent segment, it is decided according to maximum membership value. Each pixel will be assigned to the cluster containing the highest membership value comparing other clusters. Hence by sorting the clusters based on their centers absolute values in an ascending order from 1 to \hat{c} and

labeling the pixels, the **segmented image** for each land-cover will be resulted.

4.2 Analysis and Comparisons with other Segmentation Methods

Concerning input and output space (Figure 2.E), the proposed method selects all input space points and applies FCM (and consequently performing OCNDP) on one shot. Eventually, the optimum result will be among the obtained answers and can be achieved using a suitable metric and defuzzification process. Interestingly, achieving this important advantage, the computational complexity in this method would be to the order of classical methods [27,28] (one time using from clustering method and OCNDP). Classical methods [27,28] select a single point from the input space (which is equivalent to a single input image) and apply clustering method and OCNDP on that point to obtain land-cover segmentation results. It is seen the considered point from input space in these methods (and consequently the resulted outcomes) is absolutely different with the OPIS. Consequently, the obtained segmentation results would similarly differ with the actual ones (obtained results by ground experiments). From this point of view, the proposed method is a highly extended form of the classical methods. It means, the number of selected points from input space to segmentation, denoted by \hat{L} , in the classical methods is limited ($\hat{L} = 1$), but in the proposed method is unlimited ($\hat{L} \rightarrow +\infty$). Therefore, the proposed method no have classical methods defect, high distance between the optimum and resulted answer.

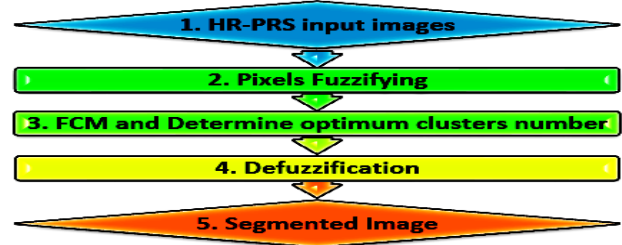


Fig. 3. The block diagram of the proposed method.

Comparing the proposed method with other multi-images segmentation methods [21-23,29-33], they apply clustering on L images or L points of input space ($\hat{L} = L$) and result output which is obtained by fusing these clustering outputs with the help of conventional fusion methods (perform fusing in the decision stage by using a known and conventional method e.g. Dempster-Shafer evidence theory). In addition to the mentioned defect of classical methods, the ambiguity in the number of optimum clusters determination (because, each input image may obtain different number in OCNDP), the way to fuse the L segmentation results and very high computational complexity (because of two reasons: 1. L times performing OCNDP applied on L input images separately while this action is time-consuming even for one time or one image; 2. Applying clustering method on

L input images) are other defects of these methods. Finally, we can summarize these comparisons as Table 1.

Eventually, it can be listed the advantages of the proposed method as follows:

1. Low computational complexity and avoiding confusion in OCNDP performing.
2. Considering OPIS as the input for segmentation and consequently obtaining the optimum response.
3. Reduction of pixels values variation effects on the segmentation results (because of the fuzzy clustering method's robustness versus the noise [41]).
4. Using various existent metrics for symbolic interval numbers [37,42-44] in the FCM applying and obtaining various correspondent responses, where each of them have their own different properties.

Capability of detecting the pixels containing high uncertainty (the land-cover points with high available values ranges). This capability can provide supervised decision about them.

4.3 New Interpretation and Comparison with Conventional Fusion Methods

In this subsection, the proposed method will compare in details with the known conventional fusion methods by mathematical analysis, where they fuse the input images and result a crisp fused image. Then the conventional FCM is applied on the resulted fused image. It must be mentioned, for simplicity, in this sub-section it is supposed $L = 2$.

In continue, firstly the performances of the conventional min, max, mean, median, OWA and Kalman-filter fusion methods are analyzed in the input space Figure 2-E, for $L = 2$. Then by proposing suitable cost functions, it will be shown that the proposed method have better performance in compare to them.

The min, max, mean and median operators (or fusion methods) have fix performance and result a fix point from the input space in the presented problem statement (input space Figure 2-E, for $L = 2$). While the location of fusion results in these methods are illustrated in Figure 4, their performances can be expressed mathematically as follows:

$$x_k = \text{Fusion}(x_k^{(1)}, x_k^{(2)}) = \text{Fusion}(x_k^{\min}, x_k^{\max}) = \begin{cases} x_k^{\min} & , \text{ if Fusion: Min} \\ x_k^{\max} & , \text{ if Fusion: Max} \\ (x_k^{\min} + x_k^{\max})/2 & , \text{ if Fusion: Mean or Median} \end{cases} \quad (15)$$

The OWA fusion method is a general form of examined methods min, max, mean and median. The OWA performance in the considered problem can be represented as follows:

$$x_k = \text{Fusion}(x_k^{(1)}, x_k^{(2)}) = wx_k^{(1)} + (1 - w)x_k^{(2)} \quad , \quad 0 \leq w \leq 1 \quad , \quad \text{if Fusion: OWA} \quad (16)$$

where the weight value w usually is satisfied by optimizing an specific cost function. For example in the availability of ground truth data $\tilde{X} = \{\tilde{x}_1, \dots, \tilde{x}_k, \dots, \tilde{x}_n\}$, the considered objective function for optimizing can be the mean


square error between the fused values $\{x_k\}_{k=1}^n$ and the actual ones $\{\tilde{x}_k\}_{k=1}^n$ as follows that must be minimized.

$$CF = \sum_{k=1}^n (x_k - \tilde{x}_k)^2 \quad (17)$$

Indeed the OWA checks the CF value for all allowed w values ($0 \leq w \leq 1$) and selects the best w value, where the CF will be optimized. This concept is equivalent to checking all points on the main diagonal of input space rectangle, point by point, and selecting the best one (as illustrated in Figure 4).

In the last case, the Kalman filter fusion method is examining. This method is as same as the OWA method with this difference that an additive white Gaussian noise has been added. The corresponding relation for this fusion method in the examining problem state is as follows:

$$x_k = \text{Fusion}(x_k^{(1)}, x_k^{(2)}) = wx_k^{(1)} + (1 - w)x_k^{(2)} + n_k, \quad 0 \leq w \leq 1 \quad , \quad n_k \sim N(0, \sigma^2), \quad \text{if Fusion: Kalman} \quad (18)$$

The resulted point set using the equation (18) is illustrated in Figure 4. It must be mentioned, the wideness of searching region (region denoted by  in Figure 4) is related to the variance of the additive noise. By increasing the variance, the wideness region will grow up and may reach to the better response; against the probability of reaching to the best point in searching region (the nearest point of search region to the OPIS) will be decreased and it will be a time-consuming process and vice versa.

Generally the set of mentioned points from the input space by these fusion methods (represented by I_{method}) can be represented by equations of (19).

It is observed, the conventional fusion methods consider a fix point (min, max, mean and median methods) or search within points on the line (the OWA method) or its around (the Kalman filter method), point by point, to get the best point in the search region. While the OPIS is not located in the search region necessarily.

Against, the proposed method consider all input space points one shot (not by search and testing point by point, as same as the examined methods) and results the best point from input space (nearest point to OPIS) as fusion method output. Therefor the set of mentioned points from the input space by proposed method can be represented as follows.

$$I_{\text{Proposed}} = I = \{x_k, \text{ for } k = 1, \dots, n \mid x_k^{\min} \leq x_k \leq x_k^{\max}\} \quad (20)$$

Comparing the mentioned points sets of introduced methods, the following equation can be concluded.

$$I_{\min}, I_{\max}, I_{\text{mean}}, I_{\text{median}} \subseteq I_{\text{OWA}} \subseteq I_{\text{Kalman}} \subseteq I_{\text{Proposed}} = I \quad (21)$$

In order to compare the various examined fusion methods, supposing availability of OPIS (ground truth data), the minimum distance achievable by each fusion method (by performing full search in OWA and Kalman) is proposed as an objective function in this paper as follows:

$$Q_{e,\text{method}} = \min \left(\sum_{k=1}^n \left\| \text{Fusion}(x_k^{(1)}, \dots, x_k^{(L)}) - \tilde{x}_k \right\|^2 \right), \quad \text{where } \text{Fusion}(x_k^{(1)}, \dots, x_k^{(L)}) \in I_{\text{method}} \quad (22)$$

Where 'method' can be referred to each examined method.

Table 1. Summarizing comparisons of the proposed method with other land-cover segmentation methods [21-23, 27-33]

Method	Property	Number of considered points from input space as input (L)	Number of performing clustering method and OCNDP	Existing the ambiguity in OCNDP for each land cover
Proposed method		$+\infty$ (contain the optimum point in input space)	1	No
other multi-images segmentation methods [21-23, 29-33]		L	L	Yes
Classical methods [27, 28]		1	1	No

$$\left\{ \begin{array}{l}
 I_{min} = \{x_k, \text{for } k = 1, \dots, n \mid x_k^{min} \leq x_k \leq x_k^{max}, x_k = x_k^{min}\} \\
 I_{max} = \{x_k, \text{for } k = 1, \dots, n \mid x_k^{min} \leq x_k \leq x_k^{max}, x_k = x_k^{max}\} \\
 I_{mean} = \{x_k, \text{for } k = 1, \dots, n \mid x_k^{min} \leq x_k \leq x_k^{max}, x_k = (x_k^{(1)} + \dots + x_k^{(L)})/L\} \\
 I_{median} = \{x_k, \text{for } k = 1, \dots, n \mid x_k^{min} \leq x_k \leq x_k^{max}, x_k = \text{median}(x_k^{(1)}, \dots, x_k^{(L)})\} \\
 I_{OWA} = \{x_k, \text{for } k = 1, \dots, n \mid x_k^{min} \leq x_k \leq x_k^{max}, x_k = w_1 x_k^{(1)} + \dots + w_L x_k^{(L)}, w_1 + \dots + w_L = 1\} \\
 I_{Kalman} = \{x_k, \text{for } k = 1, \dots, n \mid x_k^{min} \leq x_k \leq x_k^{max}, x_k = w_1 x_k^{(1)} + \dots + w_L x_k^{(L)} + n_k, w_1 + \dots + w_L = 1, n_k \sim N(0, \sigma^2)\}
 \end{array} \right. \quad (19)$$

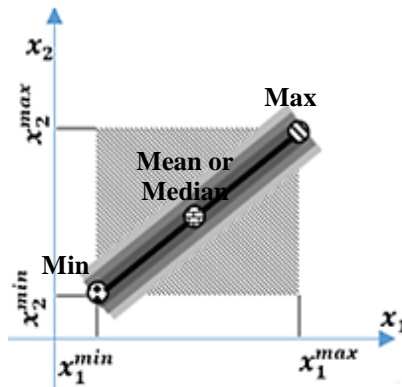


Fig. 4. The input space of multi-images segmentation and proposed method (□); resulted points by fusion methods min (●), mean (⊕), median (⊕) and max (●); resulted possible regions by fusion methods OWA (■) and Kalman (■).

Computing equation (22), independent from the exact location of \bar{X} , according to (21), following relation can be concluded:

$$Q_{e,Proposed} \leq Q_{e,Kalman} \leq Q_{e,OWA} \leq Q_{e,min}, Q_{e,max}, Q_{e,mean}, Q_{e,median} \quad (23)$$

It has been observed that the fusion result point in the proposed method is nearest to OPIS in compare to other fusion methods.

5. Simulations Results

The simulations are performed in two cases and results are reported in this section. Simulations are performed on a PC equipped with an Intel(R) core(TM) i7 cpu 960 @ 3.20GHz processor, 6GB-RAM and using Win-7 64-bits and Matlab 2012-a.

Case 1. In the first case, to subjective evaluation of the proposed method, it is applied on the images of Figure 1. Let we want to segment the corresponding land-cover of Figure 1 to 5 segments. The resulted image and corresponding labels (of mentioned region by) using

proposed method is illustrated in Figure 5. To compare it with conventional FCM, FCM is applied on the both images of Figure 1 too. Resulted images and labels of mentioned region by in this case are as Figure 6 and Figure 7. It is observed while shadow effects the resulted image by FCM in the first image (mentioned by circle), but in the proposed method result and FCM applied on the second image, shadow effect is not noticeable. Furthermore, while the proposed method obtain only one label for each point, FCM generally obtain 2 (L) various labels for each point. Generally, independent from the number of land-cover images or L , only one label is derived using proposed method for each pixel, as same as the conventional fusion ones. Against, classical methods may outcome various labels for a unique scene pixels generally. This event causes confusion in the segmentation by FCM (generally, for classical methods case).

After this subjective evaluation, in continue, the proposed method will be compared with some classical fusion based methods, such as, min, mean and max in the next section.

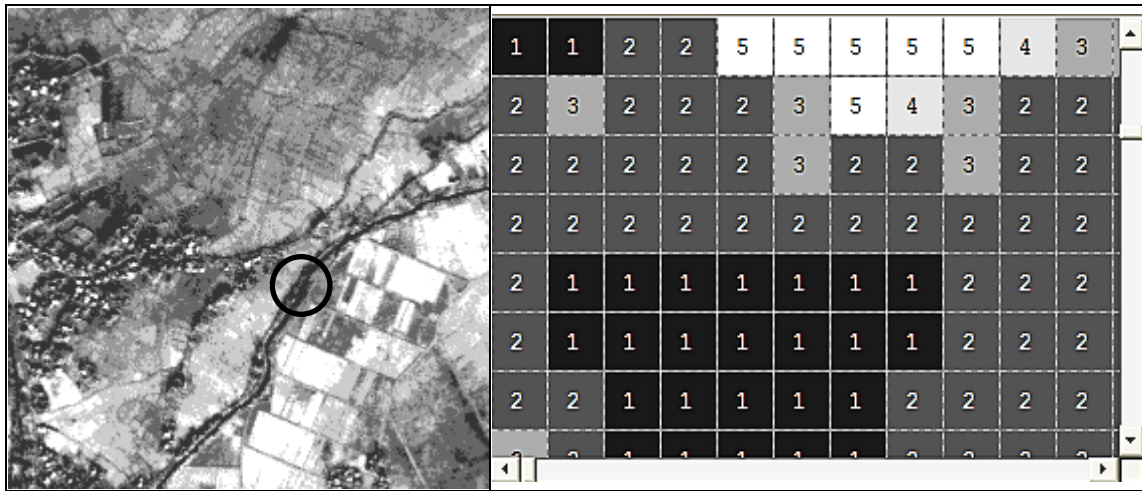



Fig. 5. The resulted image and corresponding labels of mentioned region by  in segmenting the first land-cover (Figure 1) using the proposed method.

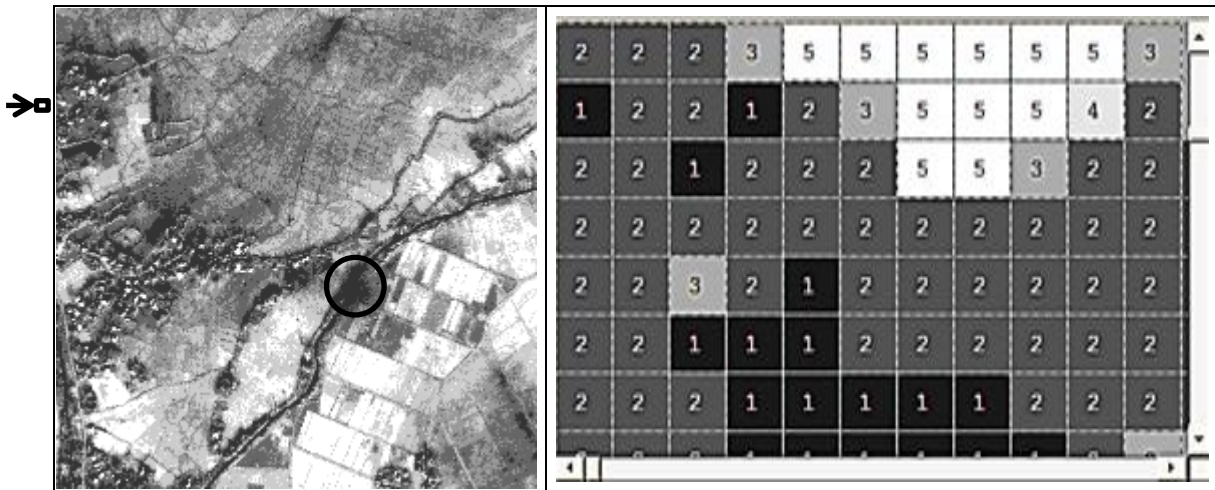



Fig. 6. The resulted image and corresponding labels of mentioned region by  in segmenting the first image of Figure 1 using the FCM.

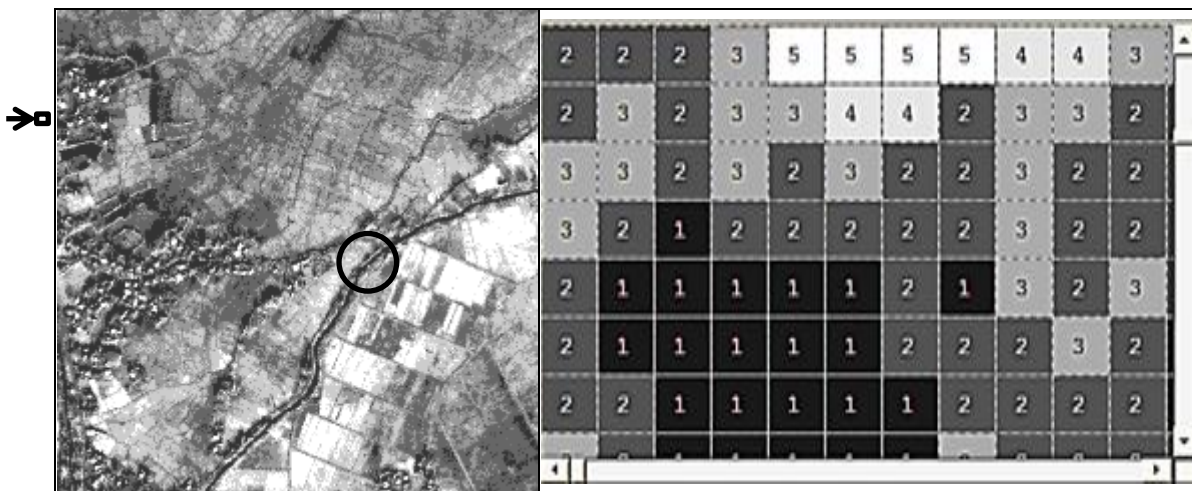



Fig. 7. The resulted image and corresponding labels of mentioned region by  in segmenting the second image of Figure 1 using the FCM.

Case 2. In this case to objective evaluation of proposed method, it is applied on the second land-cover images that are illustrated in Figure 8. This scene is located in south of Iran, with geographical location of 26.67-26.8 N and 56.04-56.06 E. Two corresponding images are obtained using Geoeey-1 (0.5 m spatial resolution) and IRS-P5 (2.5 m spatial resolution) panchromatic sensors. These images are resampled and registered together and have same size (1000*1000 pixels). In order to obtain Ground truth (GT) data for accuracy assessment, a planimetric map of this area is utilized. This map is illustrated in Figure 9-A, B.

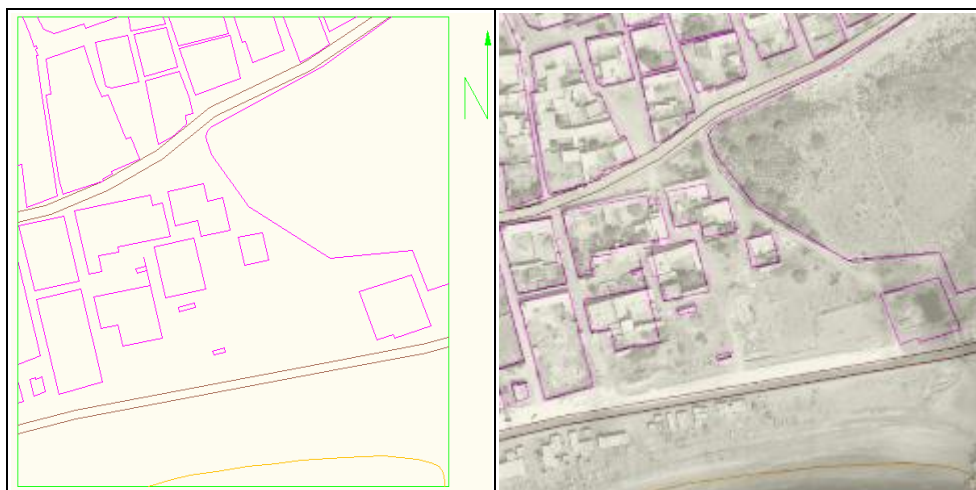
As it can be seen, the map shows exact location and structure of roads, buildings, sea, seaside and etc. While in accuracy assessment process, label of each point is needed. Therefore by using this map, on the first image of land-cover where it seems be more accurate, 4 classes (sea with black DN, main road with new and dark asphalt, sidetrack with old and bright asphalt and building's roof with white DN) are selected and labeled to 1, 2, 3 and 4 respectively, according to DN increasing manner. These 4 classes that are assumed as GT data, illustrated in Figure 9-C, D. By obtaining the GT, in continue the proposed

method will be compared objectively with classical fusion based segmentation methods. In the classical fusion based segmentation methods, named as CFSM-1, CFSM-2 and CFSM-3, the input images are fused using min, mean and max operators respectively. Then FCM is applied on the fused image, to get the segmented image. The performance of these 4 methods (proposed and 3 classical fusion based segmentation ones) are evaluated and compared together in 3 aspects. In the first case, the running time of these methods, in segmenting the land-cover to 2, 3, 4, 5 and 6 segments, are measured and reported in Table 2. It is observed that because of the random nature of methods the ranking of them is changing by change the number of segments. But it can be concluded all methods have same performance, however the proposed method has rapid convergence in the low number of segments.

In the next case study, resulted optimum number of clusters by methods is examined in Table 3 by minimizing the XB cluster validity index. Each method obtain only one number to optimum number of segments, independent from the number of input images.



Fig. 8. The second land-cover images (left: A and right: B).



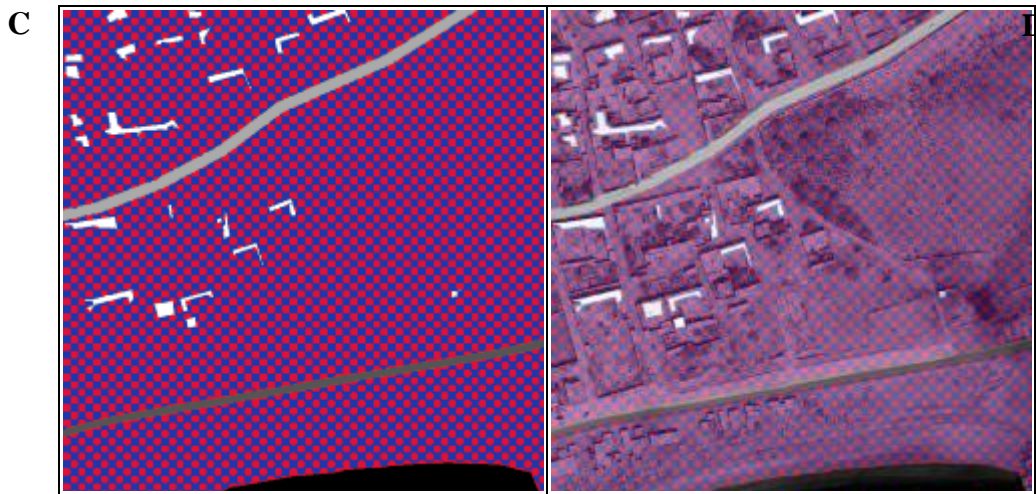


Fig. 9. A: The planimetric map of second land-cover (Figure 8); B: The planimetric map is situated on the Figure 8-A image; C: 4 classes (sea with black DN, main road with new and dark asphalt, sidetrack with old and bright asphalt and building's roof with white DN) are selected and labeled to 1, 2, 3 and 4 respectively on Figure 8-A image, other pixels are Checkered; D: Figure 9-C image is situated on the Figure 8-A image.

In the last study case, the accuracy assessment of these 4 methods and some conventional and new satellite images segmentation methods (Combination HMRF and Expectation Maximization [29], Kernel Level Set Segmentation [45], Multilevel thresholding based on Electro-magnetism Optimization [46] and Harmony Search Optimization [47], Gaussian mixture model [48] and Expectation maximization [49]) will be examined in the segmenting of land-cover to 4 segments. For this purpose, validity indices overall accuracy (OA) and Kappa (Ka) are utilized. Simulation results of this case are reported in Table 4.

It is observed, since the image Figure 8-A is influenced by shadow, furthermore, the slave roads are asphalted partially in the image Figure 8-B, the resulted segmentation by min fusion operator (CFSM-1) has the worst performance. Resulted segmentation by mean fusion operator (CFSM-2) is influenced by the mentioned error cautions (for CFSM-1 too), however less than CFSM-1. Although since the max fusion operator do not influenced by the mentioned error cautions, has the best performance. This arrangement could be inverse, if the error cautions would increase the DN of pixels, e.g. placing the region under the white cloudy dots. Against, the proposed method (PM) always has the acceptable performance, independent from the nature of error cautions. The performance of the other segmentation methods (Combination HMRF and Expectation Maximization [29], Kernel Level Set Segmentation [45], Multilevel thresholding based on Electro-magnetism Optimization [46] and Harmony Search Optimization [47], Gaussian mixture model [48] and Expectation maximization [49]) is similar to CFSM-2, because of averaging performance when they are applied on all scene images. Finally the segmented images by using the proposed and 3 classical fusion based methods are illustrated in Figure 10.

As the conclusions of simulation results, growing the RS satellites in last years, has been increased extremely the available RS data from environment. Nowadays, automatic and body-free processing and exploitation of this massive amount of data is a challenging and interesting subject. On the other hand, the images with nearby DNs to OPIS outcome good results, in the conventional segmentation methods, where they would apply only on the one single image. But there is no general method to get the image with nearby DNs to OPIS. In some regions, there is no OPIS or any knowledge to choice the image with nearest DNs to reality. Therefore, this paper proposes a new method to automatically utilizing of massive available RS data from environment and getting the good response in segmentation. However this good response will differ with obtained response by OPIS, but it is acceptable. This paper is the first work to this purpose. In the future by extending the used fuzzy numbers, metrics and etc. it is going to get the better responses, in the case of using multiple RS images.

6. Conclusions and Future Works

Land-cover segmentation using remotely sensed images is a challenging research topic. This paper proposed a method to fuse multiple panchromatic images in one fuzzy image. Finally, by applying the FCM on the resulted fuzzy image, a single segmented image was obtained for each land-cover. Some reported comparisons and mathematical analysis showed the better performance of the proposed method, in compare to the classical segmentation methods and conventional fusion methods. The performance of the proposed method also was studied when applied on two various scenes (different land-cover type). Simulation results showed the novelty and acceptable performance of the proposed method in noise-free segmentation and run

time terms. Since there is a direct relation between the performance of the proposed method and increasing the number of images for each land-cover type, in the future by obtaining more images for these land-covers, it will be tried to increase the robustness of the proposed method versus noises. Furthermore, the simplest state of non-crisp

(symbolic interval) numbers and also its simplest correspond metric were used in this paper. By improving them in the future works it will be tried to grow up the performance and efficiency.

Table 2. Running time of proposed and 3 classical fusion based segmentation methods

Method \ Num. of Seg.	2		3		4		5		6		average	
	Rank	Time	Rank	Time	Rank	Time	Rank	Time	Rank	Time	Rank	Time
PM	1	2.756	1	6.954	1	13.214	4	25.072	4	30.43	2	15.69
CFSM-1	2	5.01	2	7.4	4	16.62	2	21.78	2	26.13	1	15.39
CFSM-2	4	5.78	3	9.55	3	16.57	1	21.76	3	26.15	3	15.96
CFSM-3	3	5.64	4	11.6	2	15.65	3	21.78	1	26.05	4	16.14

Table 3. Resulted optimum number of clusters by proposed and 3 classical fusion based segmentation methods by minimizing the XB cluster validity index.

Method \ Num. of Seg.	2	3	4	5	6	Optimum
	XB	XB	XB	XB	XB	Arg min XB
PM	0.126241	0.141	0.16848	0.165728	0.144674	2
CFSM-1	0.08256	0.071798	0.074929	0.068398	0.07151	5
CFSM-2	0.091861	0.08136	0.078047	0.072338	0.075637	5
CFSM-3	0.097709	0.074982	0.07521	0.075045	0.078609	3

Table 4. Resulted overall accuracy (OA) and Kappa (Ka) indices in the accuracy assessment of proposed, 3 classical fusion based segmentation methods and 6 conventional and new satellite images segmentation methods.

Method \ Index	%OA		%Ka	
	Rank	Value	Rank	Value
PM	2	57.35	2	41.06
CFSM-1	9	56.33	10	38.25
CFSM-2	3	57.16	5	40.38
CFSM-3	1	68.27	1	56.07
[29]	8	56.53	7	39.51
[45]	4	57.15	4	40.67
[46]	10	55.78	9	38.36
[47]	5	57.11	3	40.84
[48]	6	56.67	6	39.57
[49]	7	56.58	8	39.49





Fig. 10. The resulted images in segmenting of second land-cover by using proposed (A) and 3 classical fusion based segmentation methods (B: CFSM-1, C: CFSM-2, D: CFSM-3).

References

- [1] S. Saha and S. Bandyopadhyay, "Application of a New Symmetry-Based Cluster Validity Index for Satellite Image Segmentation," *IEEE Geoscience and Remote Sensing Letters*, vol. 5, pp. 166-170, 2008.
- [2] S. Mitra, M. Dickens, and S. Pemmaraju, "Adaptive Clustering for Segmentation of Multi-sensor Images," 1998.
- [3] M. Z. Ahmed REKIK, Ahmed Ben Hamida, Mohammed Benjelloun, "Review of satellite image segmentation for an optimal fusion system based on the edge and region approaches," *International Journal of Computer Science and Network Security*, vol. 7, pp. 242-250, 2007.
- [4] I. Saha, U. Maulik, S. Bandyopadhyay, and D. Plewczynski, "SVMFC: SVM Ensemble Fuzzy Clustering for Satellite Image Segmentation," *Geoscience and Remote Sensing Letters, IEEE*, vol. 9, pp. 52-55, 2012.
- [5] G. Wang, G. Z. Gertner, S. Fang, and A. B. Anderson, "A methodology for spatial uncertainty analysis of remote sensing and GIS products," *Photogrammetric Engineering & Remote Sensing*, vol. 71, pp. 1423-1432, 2005.
- [6] C. T. Hunsaker, M. F. Goodchild, M. A. Friedl, and T. J. Case, *Spatial uncertainty in ecology: implications for remote sensing and GIS applications*: Springer Science & Business Media, 2013.
- [7] H. T. Mowrer and R. G. Congalton, *Quantifying spatial uncertainty in natural resources: theory and applications for GIS and Remote Sensing*: CRC Press, 2003.
- [8] T. Cheng, "Fuzzy objects: their changes and uncertainties," *Photogrammetric Engineering and Remote Sensing*, vol. 68, pp. 41-50, 2002.
- [9] F. Wang and G. B. Hall, "Fuzzy representation of geographical boundaries in GIS," *International Journal of Geographical Information Systems*, vol. 10, pp. 573-590, 1996.
- [10] G. Foody, "Fuzzy modelling of vegetation from remotely sensed imagery," *Ecological modelling*, vol. 85, pp. 3-12, 1996.
- [11] X. Zhao, A. Stein, and X. Chen, "Application of random sets to model uncertainties of natural entities extracted from remote sensing images," *Stochastic Environmental Research and Risk Assessment*, vol. 24, pp. 713-723, 2010.
- [12] P. Fisher, T. Cheng, and J. Wood, "Higher order vagueness in geographical information: Empirical geographical population of type n fuzzy sets," *Geoinformatica*, vol. 11, pp. 311-330, 2007.
- [13] T. Cheng and M. Molenaar, "Objects with fuzzy spatial extent," *Photogrammetric Engineering and Remote Sensing*, vol. 65, pp. 797-802, 1999.
- [14] G. Rees, *Physical principles of remote sensing vol. 1*: Cambridge Univ Pr, 2001.
- [15] E. Yasunori, T. Isao, H. Yukihiro, and M. Sadaaki, "Kernelized fuzzy c-means clustering for uncertain data using quadratic penalty-vector regularization with explicit mappings," in *Fuzzy Systems (FUZZ)*, 2011 IEEE International Conference on, 2011, pp. 804-809.
- [16] B. Kao, S. D. Lee, D. W. Cheung, W.-S. Ho, and K. Chan, "Clustering uncertain data using voronoi diagrams," in *Data Mining, 2008. ICDM'08. Eighth IEEE International Conference on*, 2008, pp. 333-342.
- [17] G. B. Heuvelink, J. D. Brown, and E. Van Loon, "A probabilistic framework for representing and simulating uncertain environmental variables," *International Journal of Geographical Information Science*, vol. 21, pp. 497-513, 2007.
- [18] X. Yu, H. He, D. Hu, and W. Zhou, "Land cover classification of remote sensing imagery based on interval-valued data fuzzy c-means algorithm," *Science China Earth Sciences*, vol. 57, pp. 1306-1313, 2014/06/01 2014.
- [19] A. Stein, N. Hamm, and Q. Ye, "Handling uncertainties in image mining for remote sensing studies," *International journal of remote sensing*, vol. 30, pp. 5365-5382, 2009.
- [20] Y. El-Sonbaty and M. A. Ismail, "Fuzzy clustering for symbolic data," *IEEE Transaction on Fuzzy Systems*, vol. 6, pp. 195-204, 1998.
- [21] S. Lee and M. Crawford, "Unsupervised classification for multi-sensor data in remote sensing using Markov random field and maximum entropy method," in *IEEE 1999 International Geoscience and Remote Sensing Symposium, 1999. IGARSS'99 Proceedings.*, 1999, pp. 1200-1202.

- [22] S. Lee, A. Suh, and M. Jung, "Multi-sensor data classification in remote sensing using MRF regional growing algorithm," in IEEE 2001 International Geoscience and Remote Sensing Symposium, 2001. IGARSS'01., 2001, pp. 2884-2886.
- [23] S. Lee and M. Crawford, "Multi-channel/multi-sensor image classification using hierarchical clustering and fuzzy classification," in IEEE 2000 International Geoscience and Remote Sensing Symposium, 2000. Proceedings. IGARSS 2000., 2000, pp. 957-959.
- [24] S. Nazarko, "Evaluation of data fusion methods using Kalman filtering and transferable belief model," Master's thesis, University of Jyväskylä, 2002.
- [25] X. Dai and S. Khorram, "Data fusion using artificial neural networks: a case study on multitemporal change analysis," *Computers, Environment and Urban Systems*, vol. 23, pp. 19-31, 1999.
- [26] H. Ghassemian, "Multisensor Image Fusion by Inverse Subband Coding," *Proceeding of ISPRS-2000*, CD, vol. 3.
- [27] M. Hasanzadeh and S. Kasaei, "A Multispectral Image Segmentation Method Using Size-Weighted Fuzzy Clustering and Membership Connectedness," *IEEE Geoscience and Remote Sensing Letters*, vol. 7, 2010.
- [28] A. A. Naeini, S. Niazmardi, S. R. Namin, F. Samadzadegan, and S. Homayouni, "A Comparison Study Between Two Hyperspectral Clustering Methods: KFCM and PSO-FCM," in *Computational Intelligence and Decision Making*, ed: Springer, 2013, pp. 23-33.
- [29] A. Bendjebbour, L. Fouque, V. Samson, and W. Pieczynski, "Multisensor Image Segmentation Using Dempster-Shafer Fusion in Markov Fields Context," *IEEE Transaction on Geoscience and Remote Sensing*, vol. 38, pp. 1789-1798, 2001.
- [30] B. Benmiloud and W. Pieczynski, "Estimation des paramètres dans les chaînes de Markov cachées et segmentation d'images," *Traitement du signal*, vol. 12, pp. 433-454, 1995.
- [31] N. Giordana and W. Pieczynski, "Estimation of generalized multisensor hidden Markov chains and unsupervised image segmentation," *IEEE Transactions on Pattern Analysis and Machine Intelligence*, vol. 19, pp. 465-475, 1997.
- [32] A. Bendjebbour and W. Pieczynski, "Multisensor Evidential Hidden Markov Fields and Image Segmentation," presented at the Second IEEE International Conference on Intelligent Processing Systems (ICIP'98), Australia, 1998.
- [33] N. Giordana and W. Pieczynski, "Unsupervised segmentation of multisensor images using generalized hidden Markov chains," in *International Conference on Image Processing*, 1996. Proceedings., 1996, pp. 987-990 vol.3.
- [34] M. S. Balch, "Methods for Rigorous Uncertainty Quantification with Application to a Mars Atmosphere Model," Virginia Polytechnic Institute and State University, 2010.
- [35] M. Hadi, K. Morteza, and S. Y. Hadi, "Vector fuzzy C-means," *Journal of Intelligent and Fuzzy Systems*, vol. 24, pp. 363-381, 2013.
- [36] K. L. Wu and M. S. Yang, "Alternative c-means clustering algorithms," *Pattern Recognition*, vol. 35, pp. 2267-2278, 2002.
- [37] C. C. Chuang, J. T. Jeng, and C. W. Li, "Fuzzy C-Means Clustering Algorithm with Unknown Number of Clusters for Symbolic Interval Data," presented at the SICE Annual Conference, 2008.
- [38] S. Saha and S. Bandyopadhyay, "Application of a Multiseed-Based Clustering Technique for Automatic Satellite Image Segmentation," *IEEE Geoscience and Remote Sensing Letters*, vol. 7, pp. 306-308, 2010.
- [39] S. Das and S. Sil, "Kernel-induced fuzzy clustering of image pixels with an improved differential evolution algorithm," *Information Sciences*, vol. 180, pp. 1237-1256, 2010.
- [40] X. L. Xie and G. Beni, "A validity measure for fuzzy clustering," *IEEE Transactions on pattern analysis and machine intelligence*, vol. 13, pp. 841-847, 1991.
- [41] S.-B. Cho and S.-H. Yoo, "Fuzzy Bayesian validation for cluster analysis of yeast cell-cycle data," *Pattern recognition*, vol. 39, pp. 2405-2414, 2006.
- [42] P. D'Urso and P. Giordani, "A weighted fuzzy c-means clustering model for fuzzy data," *Computational Statistics & Data Analysis*, vol. 50, pp. 1496-1523, 2006.
- [43] F. A. T. D. Carvalho, "Fuzzy clustering algorithms for symbolic interval data based on adaptive and non-adaptive Euclidean distances," in *Proceedings of the Ninth Brazilian Symposium on Neural Networks (SBRN'06)*, 2006, pp. 60-65.
- [44] F. A. T. D. Carvalho, "Fuzzy c-means clustering methods for symbolic interval data," *Pattern Recognition Letters*, vol. 28, pp. 423-437, 2007.
- [45] M. Ben Salah, A. Mitiche, and I. Ben Ayed, "Effective level set image segmentation with a kernel induced data term," *Image Processing, IEEE Transactions on*, vol. 19, pp. 220-232, 2010.
- [46] D. Oliva, E. Cuevas, G. Pajares, D. Zaldivar, and V. Osuna, "A Multilevel Thresholding algorithm using electromagnetism optimization," *Neurocomputing*, vol. 139, pp. 357-381, 2014.
- [47] D. Oliva, E. Cuevas, G. Pajares, D. Zaldivar, and M. Perez-Cisneros, "Multilevel thresholding segmentation based on harmony search optimization," *Journal of Applied Mathematics*, vol. 2013, 2013.
- [48] H. Greenspan, A. Ruf, and J. Goldberger, "Constrained Gaussian mixture model framework for automatic segmentation of MR brain images," *Medical Imaging, IEEE Transactions on*, vol. 25, pp. 1233-1245, 2006.
- [49] M. L. Comer and E. J. Delp, "The EM/MPM algorithm for segmentation of textured images: Analysis and further experimental results," *Image Processing, IEEE Transactions on*, vol. 9, pp. 1731-1744, 2000.

Hadi Mahdipour Hossein-Abad was born in Shirvan, Iran, in 1984. He received the B.S. degree in electrical engineering (Communication trend) from Ferdowsi University of Mashhad, Iran, in 2005. Then he received the M.S. degree in electrical engineering (Communication trends) from Shahid Bahonar University of Kerman, Iran, in 2007. Finally he received the Ph.D. degree in electrical engineering (Communication-system trend) from Ferdowsi University of Mashhad, Iran, in 2010. He is currently Assistant Professor at Faculty of Marine Engineering, Khorramshahr University of Marine Science and Technology, Iran, from 2010. His research interests include pattern recognition, image and video processing and telecommunication. Email: mahdipour@kmsu.ac.ir.

Morteza Khademi was born in Iran, in 1958. He received the B.Sc. and M.S. degrees from Isfahan University of Technology, Isfahan, Iran, in 1985 and 1987, respectively and the Ph.D. degree from the Wollongong University, Australia, on video communications in 1995, all in Electrical Engineering. He joined Ferdowsi University of Mashhad, Iran in 1987. He is currently Professor at the Department of Electrical Engineering, Ferdowsi University of Mashhad, Iran. His research interests include image and video processing and communication and biomedical signal processing. Email: khademi@um.ac.ir.

Hadi Sadoghi Yazdi received the B.S. degree in electrical engineering from Ferdowsi University of Mashhad, Iran in 1994, and then he received to the M.S. and PhD degrees in electrical engineering from Tarbiat Modarres University of Tehran, Iran, in 1996 and 2005 respectively. He works in Computer Department

as a professor at Ferdowsi University of Mashhad. His research interests include adaptive filtering, image and video processing, and optimization in signal processing. Email: h-sadoghi@um.ac.ir.